

## SUPPORTING INFORMATION

# Near-infrared random lasing realized in solution-processed perovskite thin film

Zhi-Feng Shi,<sup>\*a</sup> Xu-Guang Sun,<sup>a</sup> Di Wu,<sup>a</sup> Ting-Ting Xu,<sup>a</sup> Yong-Tao Tian,<sup>a</sup> Yuan-Tao Zhang,<sup>b</sup>  
Xin-Jian Li<sup>\*a</sup> and Guo-Tong Du<sup>b</sup>

<sup>a</sup>Department of Physics and Laboratory of Material Physics, Zhengzhou University, Daxue Road 75, Zhengzhou 450052, China

<sup>b</sup>State Key Laboratory on Integrated Optoelectronics, College of Electronic Science and Engineering, Jilin University, Qianjin Street 2699, Changchun 130012, China

---

<sup>\*</sup>Author to whom correspondence should be addressed. Electronic mail: shizf@zzu.edu.cn; lixj@zzu.edu.cn

## **Investigation on the phase coexistence phenomenon of $\text{CH}_3\text{NH}_3\text{PbI}_3$ thin film**

As shown in Figure S1, we performed the temperature-dependent XRD measurements at three typical temperature points (300, 160, and 77 K) to support our findings from PL spectra. At 300 K, the diffraction peaks at  $14.35^\circ$ ,  $28.66^\circ$ , and  $43.18^\circ$  could be assigned to the (110), (220), and (330) planes of crystalline  $\text{CH}_3\text{NH}_3\text{PbI}_3$ , suggesting the formation of a tetragonal perovskite structure (space group  $I4/mcm$ ). At 160 K (structural phase transition temperature stated in the manuscript), some emerging diffraction peaks at  $14.19^\circ$ ,  $28.36^\circ$ ,  $31.62^\circ$ , and  $41.10^\circ$  can be observed, corresponding to (101), (202), (301), and (242) diffractions of orthorhombic structure. Obviously, the existence of residual tetragonal phase implies an incomplete phase transition of  $\text{CH}_3\text{NH}_3\text{PbI}_3$  product. More importantly, such a phase coexistence phenomenon still exists although the measurement temperature is as low as 77 K. The temperature-dependent XRD results match well with the findings in temperature-dependent PL shown in the manuscript.

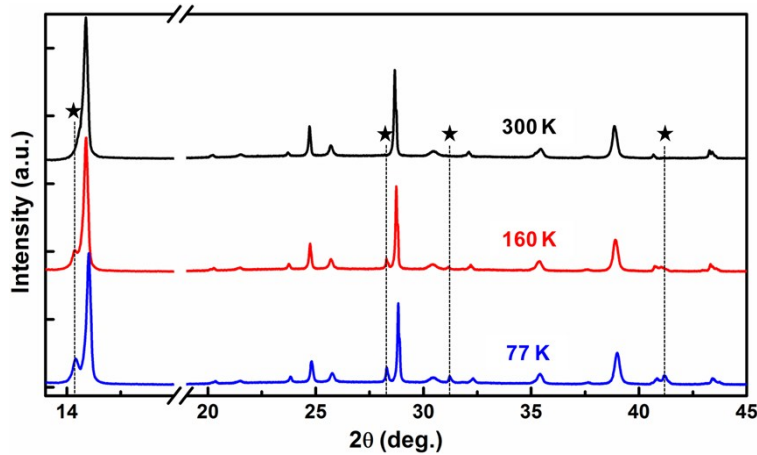


Figure S1. XRD patterns of the  $\text{CH}_3\text{NH}_3\text{PbI}_3$  thin film at three typical temperatures. The asterisk is used to identify the appearance of orthorhombic phase.

## **Gaussian deconvolution of the PL spectra at different temperatures**

Low-temperature photoluminescence (PL) at three typical temperature points were put together for a better comparison because the carrier recombination processes were changed with temperature. As shown in Figure S2, three PL spectra at 77, 90, and 100 K could be resolved into three components, centered at around 748, 780, and 811 nm, respectively. The component on the high-energy side ( $\sim 748$  nm, R-1) is attributed to the low-temperature orthorhombic phase. The medium component at  $\sim 780$  nm (R-2) is associated with the high-temperature tetragonal phase. And the component on the low-energy side ( $\sim 811$  nm, R-3) can be ascribed to the trap-mediated radiative recombination. Obviously, with the decrease of temperature, the contribution of carrier recombination channel from R-1 increases gradually, while the opposite is the case for R-2. Specifically, the relative percentages ( $\eta\%$ ) of R-1 for the PL spectra at three temperature points are 12.25%, 7.79%, and 5.27%, respectively, as summarized in Table 1.

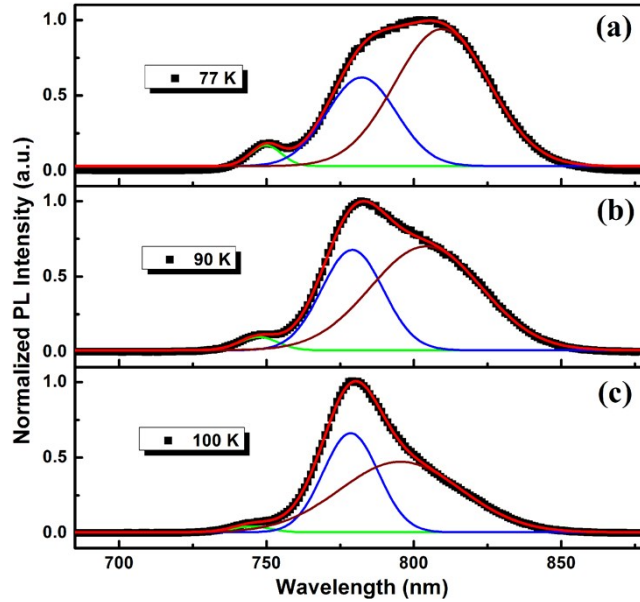


Figure S2. Gaussian deconvolution of the PL spectra measured at (a) 77, (b) 90, and (c) 100 K, respectively.

### **Relative percentages of three recombination channels in $\text{CH}_3\text{NH}_3\text{PbI}_3$ film at different temperatures**

Temperature	Parameters	R-1	R-2	R3
77 K	Wavelength (nm)	749	782	812
	$\eta$ %	12.25	30.40	57.35
90 K	Wavelength (nm)	748	779	807
	$\eta$ %	7.79	34.87	55.34
100 K	Wavelength (nm)	746	778	779
	$\eta$ %	5.27	40.37	54.36

Table S1. Detailed data from the Gaussian deconvolution of PL spectra at different temperatures

### **Analysis of the carrier recombination mechanisms of $\text{CH}_3\text{NH}_3\text{PbI}_3$ thin film**

The PL spectrum of  $\text{CH}_3\text{NH}_3\text{PbI}_3$  thin film at 77 K was taken as the research object to further investigate its carrier recombination mechanism. As shown in Figure S3, the PL spectrum

can be well-fitted by three Gaussian peaks, and each emission band corresponds to a particular recombination process, as described above.

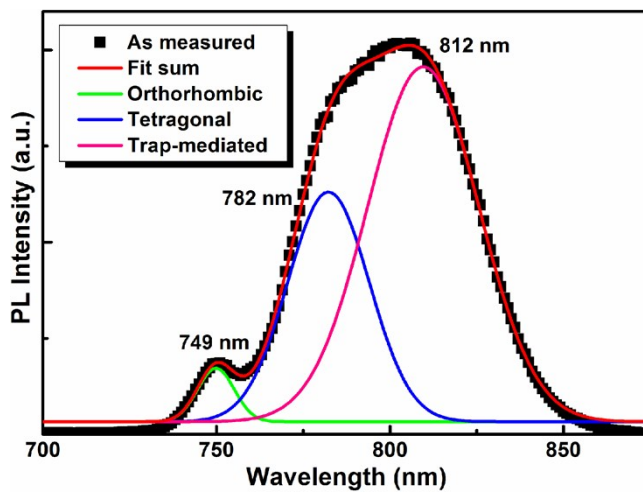


Figure S3. Gaussian deconvolution of the PL spectrum measured at 77 K showing three different carrier recombination channels.

### **Lineshape analysis of $\text{CH}_3\text{NH}_3\text{PbI}_3$ thin film at 77 K**

As shown in Figure S4, the steady-state PL spectrum measured at room-temperature with the excitation power of 3.0 mW can be fitted with two components, exciton-related emission

(Gaussian, blue) plus free carrier-related emission (Gaussian, green). In addition, the ratio of free carrier-related emission to exciton-related emission is calculated to be  $\sim 7.2\%$ .

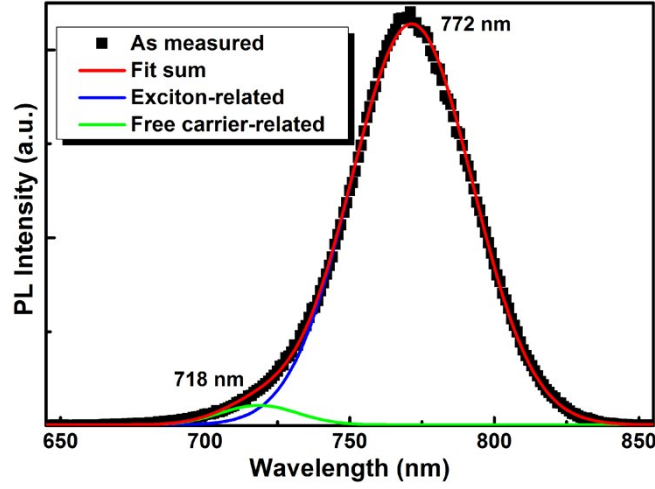


Figure S4. Gaussian deconvolution of the steady-state PL spectrum measured at room-temperature with the excitation power of 3.0 mW, showing the exciton-related emission and free carrier-related emission.

### **Excitation power-dependent PL intensity of $\text{CH}_3\text{NH}_3\text{PbI}_3$ thin film at 170 K**

Figure S5 shows the relationship between the integrated PL intensity and the excitation power measured at 170 K. The obtained data was fitted by the equation of  $I_{\text{PL}} = I_{\text{EX}}^\beta$ , where  $\beta$

denotes the nonlinear component. By fitting the experimental data, a superlinear relation with  $\beta \sim 1.20$  held the curve, smaller than the value ( $\sim 1.29$ ) derived at room-temperature.

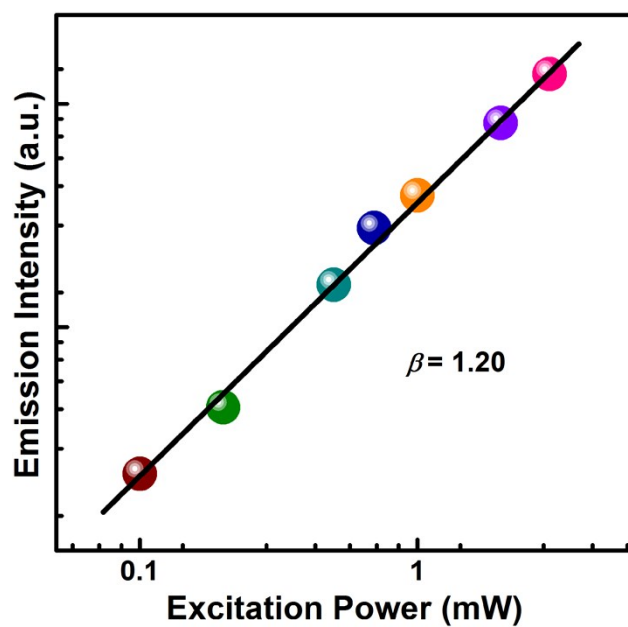


Figure S5. The relationship between the integrated PL intensity and the excitation power measured at 170 K.